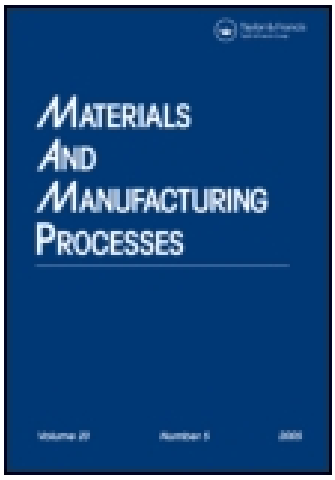

Materials and Manufacturing Processes
Publication details, including instructions for authors and subscription information:
http://www.tandfonline.com/loi/lmmp20

Use of Welding-Brazing Technology on Microstructural Development of Titanium/Aluminum Dissimilar Joints

Shouzheng Wei [a], Yajiang Li [a], Juan Wang [a] & Kun Liu [a]
[a] Key Laboratory for Liquid-Solid Structural Evolution and Processing of Materials (Ministry of Education), Shandong University, Jinan, P. R. China
Published online: 18 Jul 2014.

To cite this article: Shouzheng Wei, Yajiang Li, Juan Wang & Kun Liu (2014) Use of Welding-Brazing Technology on Microstructural Development of Titanium/Aluminum Dissimilar Joints, Materials and Manufacturing Processes, 29:8, 961-968, DOI: 10.1080/10426914.2014.921711

To link to this article: http://dx.doi.org/10.1080/10426914.2014.921711

Materials and Manufacturing Processes, 29: 961–968, 2014

ISSN: 1042-6914 print/1532-2475 online
DOI: 10.1080/10426914.2014.921711

Taylor & Francis
Taylor & Francis Group

Use of Welding–Brazing Technology on Microstructural Development of Titanium/Aluminum Dissimilar Joints

Shouzheng Wei, Yajiang Li, Juan Wang, and Kun Liu

Key Laboratory for Liquid-Solid Structural Evolution and Processing of Materials (Ministry of Education), Shandong University, Jinan, P. R. China

A novel gas tungsten arc welding–brazing technology was utilized to butt weld titanium Ti-6Al-2Zr-Mo-1.5V to aluminum Al-5Mg-0.6Mn dissimilar alloys using AlSi5 filler metal. Microstructures of the weld zone were analyzed using optical microscopy and scanning electron microscopy. Phase constitution in the reaction zone was characterized by means of X-ray diffraction and energy-dispersive X-ray spectroscopy. The results showed that joint with good appearance can be obtained using the welding–brazing technology. A fusion zone with α-Al and α-Al + Mg_2Si + silicon eutectic structure was formed at the aluminum side. Top surface of the titanium was partially melted and a thin titanium/aluminum fusion zone was formed between titanium and weld metal. In other regions, titanium and aluminum were brazed together by the formation of an unequal-thickness reaction layer. Five different intermetallic layers with $Ti_{3.3}Al$, $Ti_{3.3}Al + Ti_5Si_3$, $TiAl + Ti_5Si_3$, $TiAl_2 + Ti_5Al_{11} + Ti_9Al_{23} + Ti_5Si_3$, and $TiAl_3$ are observed orderly from titanium to the weld metal in the titanium/aluminum fusion zone. Two intermetallic layers with $Ti_7Al_5Si_{12}$ and $TiAl_3$ are observed near the titanium/aluminum-brazed interface.

Keywords Aluminum; Brazing; Intermetallics; Microstructures; Titanium; Welding.

Introduction

Joining of titanium to aluminum has increasing significance in aviation and space applications owing to the increasing demand of lightweight components with high strength. Melting points of titanium and aluminum are 1667°C and 660°C, respectively. The wide difference between these two materials leads to the difficulty in thermal joining them by conventional fusion welding. Moreover, titanium and aluminum were previously thought to have limited weldability due to the formation of brittle intermetallics [1]. Welding cracks initiate easily in the thick intermetallic layers [2, 3]. Fusion welding of titanium Ti-6Al-4V to aluminum Al-Mg-0.9Si was investigated in reference [4] using laser beam welding, and brittle intermetallics (mainly TiAl and $TiAl_3$) were formed in the fusion zone. Most researches have focused on solid state welding technologies such as brazing [5, 6], diffusion bonding [7, 8], and friction stir welding [9, 10] to prevent forming of too many intermetallics.

The concept of introducing a novel welding–brazing technology into joining titanium to aluminum has been put forward; joints without cracks were produced using laser beam welding [11]. Formation of thick intermetallic layers would degrade joint properties for having a high cracking sensitivity. It is important to improve the interfacial microstructures by controlling the welding heat input at a low degree. The welding–brazing process, which is fusion welding for the material with low melting point and brazing for the material with high melting point, could prevent melting of too much titanium, thereby reduce the formation of intermetallics. A rectangular laser beam was utilized in welding–brazing of titanium to aluminum, and joints with sound properties were observed in a proper welding heat input range [1]. Tensile strength and resistance to fatigue cracking of the welded–brazed titanium/aluminum joints were improved by making a U-slot groove in aluminum [12].

Gas tungsten arc welding has wide applications, and researches on welding–brazing of titanium to aluminum were conducted using this welding technology. A novel keyhole gas tungsten arc welding–brazing process was utilized in butt joining of titanium to aluminum [13], microstructure of the weld zone was improved, and the tensile strength of the joint reached 270 MPa. As brittle intermetallics do harm to the joint properties, attempts were conducted to suppress the formation of intermetallics. AlSi12 filler metal was used in gas tungsten arc welding–brazing of titanium to aluminum, a thin $Ti(Al, Si)_3$ layer was formed near the interface, and the transverse strength of the joint was higher than that of the aluminum [14]. Butt welding–brazing of titanium to aluminum using AlSi12 filler metal without flux was investigated in reference [15], and reaction layers with needle-like $Ti_7Al_5Si_{12}$ and serrate $Ti(Al, Si)_3$ were formed near the titanium/aluminum interface.

Received March 11, 2014; Accepted April 4, 2014

Address correspondence to Yajiang Li and Juan Wang, Key Laboratory for Liquid-Solid Structural Evolution and Processing of Materials (Ministry of Education), Shandong University, Jinan 250061, P. R. China; E-mail: yajli@sdu.edu.cn; jwang@sdu.edu.cn.

Color versions of one or more of the figures in the article can be found online at www.tandfonline.com/lmmp.

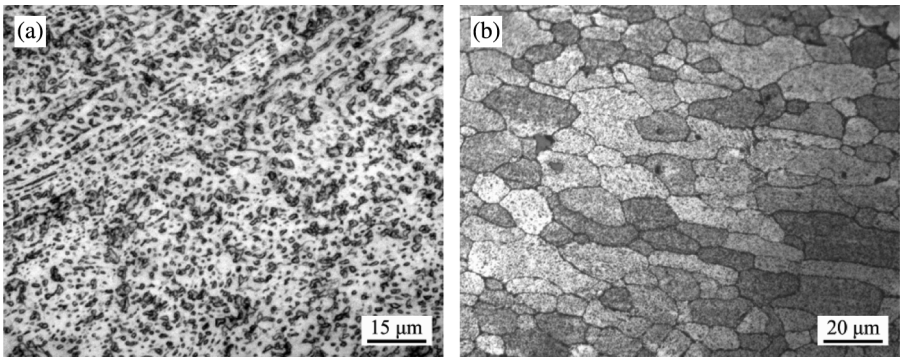

FIGURE 1.—Microstructures of base metals: (a) titanium Ti-6Al-2Zr-Mo-1.5V and (b) aluminum Al-5Mg-0.6Mn.

It seems that intermetallics could not be eliminated during gas tungsten arc welding–brazing of titanium to aluminum according to researches above. As intermetallic layers play an important role in the fracture of the titanium/aluminum joint, it is important to investigate the phase constitution in the joint. In the present study, butt gas tungsten arc welding–brazing of titanium to aluminum was conducted using aluminum–silicon filler metal. Microstructures and microhardness distribution in the welded joint were analyzed in detail. Phase constitution in titanium/aluminum reaction zone was also studied.

EXPERIMENTAL PROCEDURES

The rolled near-α titanium Ti-6Al-2Zr-Mo-1.5V and annealed rust-proof aluminum Al-5Mg-0.6Mn were used as base metals. Microstructures of base metals are shown in Fig. 1. The titanium has a microstructure with orientation α phase decorated with β phase. The aluminum is composed of α-Al(Mg) grains and β (Al_3Mg_2) phase precipitations. The welding specimens were cut from matrix and machined to sheets with dimensions of 200 mm × 50 mm × 2.5 mm. The silicon has an apparent effect in restricting the formation of intermetallics based on former researches [16, 17]. However, adding of too much silicon would results in the formation of brittle eutectic structure α-Al(Mg) + Mg_2Si Si in the fusion zone near aluminum [18]. So the AlSi5 wire with diameter of Φ2.0 mm was used as filler metal. Chemical compositions of base metals and filler metal are listed in Table 1.

All the sheets need strictly cleaned before welding. Surfaces of titanium were cleaned using acidic solution (HNO_3 20 vol%, HF 2 vol%, H_2O 78 vol%). Surfaces of aluminum were cleaned using alkali liquor (NaOH 8 vol%, H_2O 92 vol%). The joining surfaces were ground with 1000 grit SiC paper. All the sheets were ultrasonic cleaned in acetone solution and then dried.

The welding was carried out using WES-250P square-wave alternating current gas tungsten arc welding source (Chaosheng, Guangzhou, China); the diameter of tungsten electrode was Φ 2.4 mm. The joint was arranged in the pattern of "Y" with narrow gap to improve the spreadability of liquid filler metal, and the bevel angle was 30° in titanium. Main geometrical parameters of the welding are shown in Fig. 2(a). The welding parameters were as follows: striking current of 60 Å, welding current of 100–110 Å, crater current of 40 Å, arc voltage of 11–12 V, and welding rate of 0.10 ± 0.01 m/min. The frequency of alternating current was 50 Hz. The filler wire was fed by hand. The welding was carried out in a device full of argon shield gas without preheating the specimens. The argon flow rate was 16 L/min. The joints were cooled down in the argon atmosphere after welding.

Standard grind and polish procedure was adopted to prepare cross-sectional samples. The samples were chemically etched with etchant (HF 15 vol%, HNO_3 15 vol%, and H_2O 70 vol%) between 5 and 10 s. Microstructures of the weld zone were observed using optical microscopy (OM) and HITACHI SU-70 field emission scanning electron microscopy (FE-SEM) (Hitachi, Japan). Microhardness measurement was performed using DHV-1000 microsclerometer with a load of 0.05 kg. Both the dwell and unloading durations were 10 s. Distances between two neighboring indentations in titanium and in aluminum were 50 μm and 100 μm, respectively.

X-ray diffraction (XRD) was utilized to investigate the phase constitution in the titanium/aluminum reaction zone. A modified method was adopted in the study

TABLE 1.—Chemical compositions of base metals and filler metal.

Materials	Ti	Al	Si	V	Mg	Mo	Zr	Fe	Cu	Zn	Mn
Titanium	Bal.	6.50	0.10	1.80	—	1.00	2.00	0.10	—	—	—
Aluminum	0.04	Bal.	0.40	—	6.20	—	—	0.40	0.10	0.20	0.55
Filler metal	—	Bal.	5.5	—	0.05	—	—	0.80	0.30	0.10	0.05

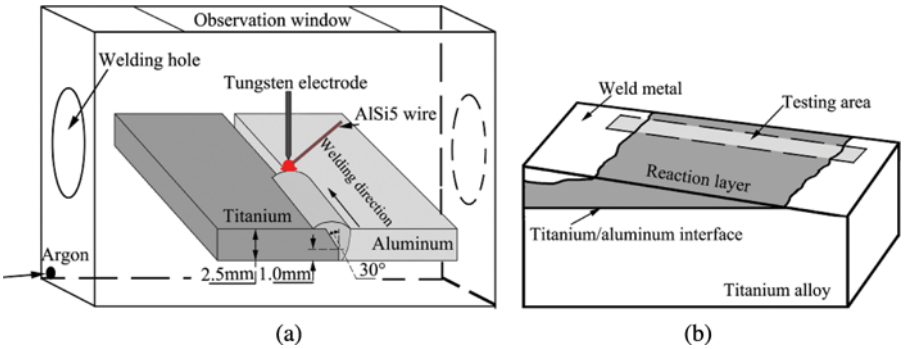

FIGURE 2.—Schematic drawing of experiments: (a) gas tungsten arc welding and (b) samples for X-ray diffraction.

as shown in Fig. 2(b). An inclined testing surface was machined from the weld metal to titanium crossing the reaction zone. The accuracy of analysis is raised by increasing the testing area. To study the distribution order of phases in the reaction zone, chemical compositions of the reaction zone were analyzed using a HORIBA EX-250 energy-dispersive X-ray spectroscopy (EDS) (Horiba, Japan).

RESULTS AND DISCUSSION

Joint Appearance and Macrostructure

A good weld appearance is obtained using the gas tungsten arc welding–brazing as shown in Fig. 3(a). Titanium was well wetted by the molten filler metal giving a consistent joint on both sides. Surface of the weld metal is smooth. No macroscopic cracking is observed in the top surface and bottom of the joint. Widths of the upper side and bottom of the weld metal are 9.0 ± 1.0 and 4.0 ± 0.5 mm, respectively.

Metallographic samples perpendicular to welding direction were sectioned from the joint, as shown in Fig. 3(b). Dual characteristics of fusion welding and brazing are exhibited in the joint. A fusion zone is observed at the aluminum side. For the titanium side, the filler metal had spread fully on the surface of titanium to form a good front and back joining. The titanium/aluminum reaction zone on the top surface takes a wavy appearance. It is a sign that the top surface of titanium was partially melted. Sharp titanium/aluminum interfaces are observed in other regions. Furthermore, heat-affected zones are easily observed both in titanium and aluminum.

During the welding–brazing process, AlSi5 filler metal was melted due to the direct heating by the welding arc. Temperature of molten filler metal exceeded the melting temperature of aluminum. The aluminum base metal was partially melted and mixed with the liquid filler metal. Also, a fusion zone was formed between the aluminum and weld metal. Because temperature of liquid filler metal on the top surface was a little higher than the melting temperature of titanium alloy, titanium was melted slightly and a wavy reaction zone was formed. In other regions, temperature of liquid filler metal is below the melting temperature of titanium, the titanium was stayed in solid state during the welding–brazing, and sharp titanium/aluminum-brazed interface was formed between titanium and the weld metal. Thus different reaction zones were formed between the titanium and weld metal due to the inhomogeneous distribution of welding heat input along the thickness direction.

Microstructure of Fusion Zone Near Aluminum

Microstructure of fusion zone near aluminum is shown in Fig. 4(a). No defects such as voids or pores are observed near the fusion zone. A columnar grain zone that is nearly vertical to the fusion line is observed between the weld metal and heat-affected zone of aluminum. The fusion zone is composed of columnar grains and boundary structures. Chemical compositions of the boundary structures were analyzed using EDS. Test locations 1, 2, and 3 are shown in Fig. 4(b). Atomic weight of aluminum in location 1 is 98.2 at%, it is clear that the grain is α-Al solution. Atomic weights of

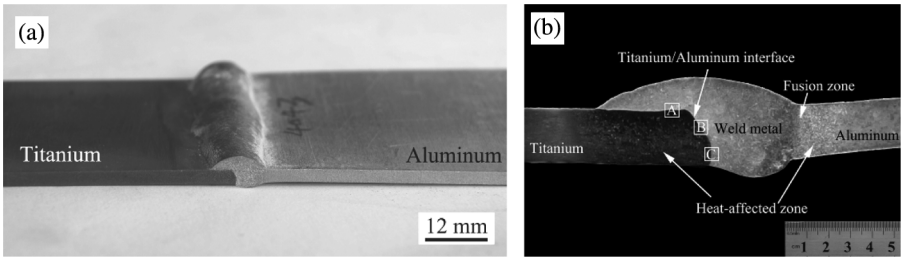

FIGURE 3.—Appearance and cross section of the titanium/aluminum joint: (a) joint appearance and (b) cross section.

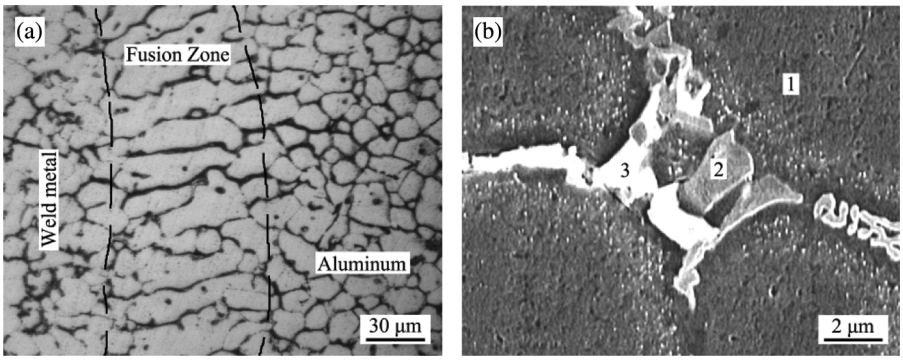

FIGURE 4.—Microstructure of fusion zone at aluminum side: (a) OM micrograph and (b) test locations of EDS.

aluminum, silicon, and magnesium in location 2 are 30.5 at%, 67.2 at%, and 2.3 at%, respectively. The result indicates that the gray block is mainly composed of silicon. Atomic weights of silicon and magnesium in location 3 are 20.4 at%, 38.0 at%, respectively. The bright phase may be the Mg_2Si according to aluminum–silicon–magnesium phase diagram. Thus phases around α-Al grains are ternary eutectic structures of α-Al + Mg_2Si + silicon. A few globular precipitations distribute in the columnar grains. The precipitations were revealed as β (Al_3Mg_2) phase using EDS.

Based on observations above, aluminum was partially melted and mixed with liquid filler metal during the welding–brazing process. Aluminum, silicon, and magnesium were rich elements in the liquid metal near the aluminum alloy. The solid–liquid interface provided heterogeneous nucleation condition for crystallization of the liquid metal during the cooling process. A high temperature gradient vertical to the solid–liquid interface occurred due to the high heat conduction ability of aluminum. Priority crystallization of the liquid metal was along the direction of temperature gradient, which resulted in the formation of a columnar grain zone in the fusion zone. Because concentrations of silicon and magnesium were lower than 5.0 wt% in the liquid metal, α-Al(Si, Mg) crystallized first during the cooling process according to aluminum–silicon–magnesium ternary phase diagram. Concentrations of silicon and magnesium in the liquid metal ascended with the crystallization of α-Al grains. Composition of the liquid metal approached to the eutectic point of aluminum–silicon–magnesium in the end, and eutectic structure α-Al + Mg_2Si + silicon were formed on the boundaries of α-Al grains. In the columnar grains, all the β (Al_3Mg_2) phases were decomposed and dissolved into α-Al solid solution due to the weld thermal cycle [18]. Only a few β phases were formed as globular precipitations owing to actions between aluminum and magnesium.

Phase Constitution Near the Titanium/Aluminum Reaction Zone

Optical micrographs of weld zone near the titanium at different locations that are marked as A–C zones in Fig. 3(b) are shown in Fig. 5. A visible unequal-thickness reaction zone is observed between the titanium and weld metal. Top surface of titanium was partially melted as shown in Fig. 5(a). A fusion zone with thickness of 18.0 ± 2.0 μm and a large number of discrete precipitations are observed in Zone A. Chemical composition of precipitations was examined using EDS, atomic weights of titanium and aluminum are 25.5 at% and 68.2%, respectively. Thus the precipitations are mainly composed of $TiAl_3$. Titanium was not melted in Zone B. A reaction layer with thickness of 7.0 ± 1.0 μm is observed near the interface, and the number of $TiAl_3$ precipitations in the weld metal is less than that in Zone A, as shown in Fig. 5(b). The thickness of the reaction layer

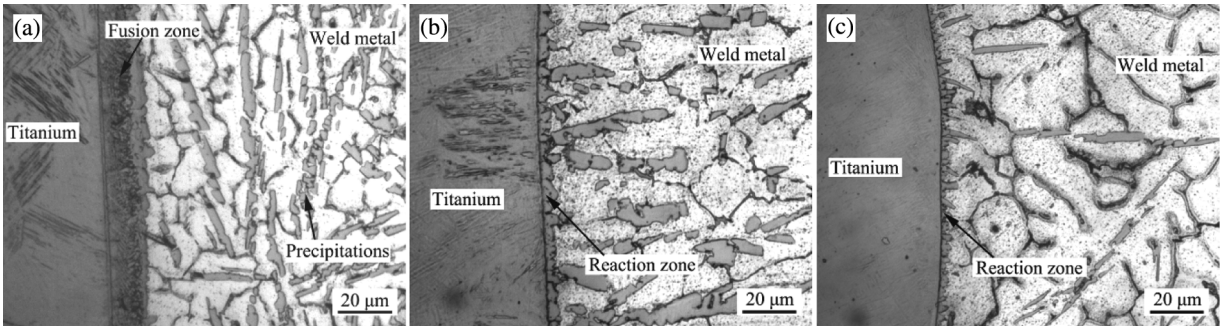

FIGURE 5.—Microstructure of titanium/aluminum reaction zone along thickness direction (a) A zone in Fig.3, (b) B zone in Fig.3, (c) C zone in Fig. 3.

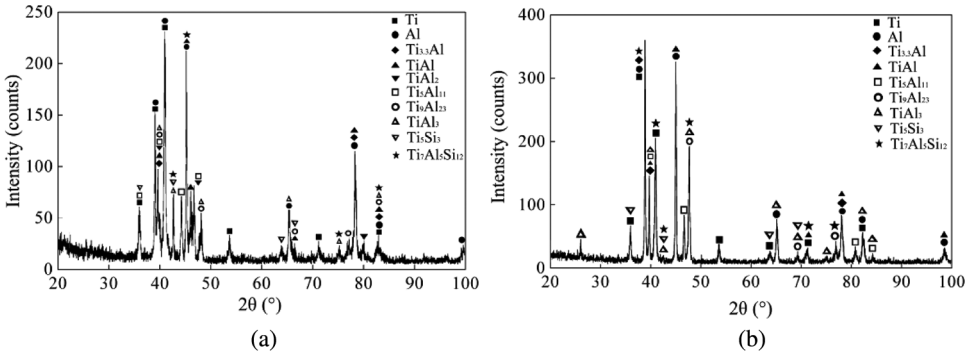

FIGURE 6.—X-ray diffraction profiles near the titanium/aluminum reaction zone.

in Zone C is approximately 3.0 μm, as shown in Fig. 5(c). There are only a few $TiAl_3$ in the weld metal in Zone C.

In order to analyze the phase constitution near the titanium/aluminum reaction zone, samples with different positions were examined by means of XRD. The test results are shown in Fig. 6. Several kinds of intermetallics including $Ti_{3.3}Al$, TiAl, $TiAl_2$, Ti_5Al_{11}, Ti_9Al_{23}, $TiAl_3$, Ti_5Si_3, and $Ti_7Al_5Si_{12}$ are observed in the reaction layers under the gas tungsten arc welding–brazing condition. The test results are different from observations in the former researches [4, 16].

Both fusion zone and brazed interface are observed between titanium and weld metal. Phase constitution near the brazed interface had been discussed in other contribution [19]; intermetallic layers with $Ti_7Al_5Si_{12}$ and $TiAl_3$ were formed between titanium and weld metal, and it is important to analyze the phase constitution in the fusion zone. SEM micrographs of the titanium/aluminum fusion zone are shown in Fig. 7. The detailed microstructures of Zones A and B that marked by squares in Fig. 7(a) are shown in Figs. 7(b) and (c), respectively. The fusion zone is divided into several layers that marked as I, II, III, IV, and V in Figs. 7(b) and (c).

In order to analyze the distribution order of intermetallics in the fusion zone, chemical compositions of selected locations that marked as 1–6 in Fig. 7 were analyzed using EDS. The results are listed in Table 2. In location 1, atomic weights of titanium and aluminum are 86.62 at% and 10.83 at%, respectively. The results indicate that the region is titanium base metal with a small dissolution of aluminum. In location 2, atomic weights of titanium and aluminum are 72.81 at% and 24.16 at%, respectively. The atomic ratio of titanium to aluminum is approximately 3:1. The layer I is composed of $Ti_{3.3}Al$ based on observations of XRD. Atomic ratio of titanium to aluminum is approximately 3:1 in location 3, and the layer II is mainly composed of $Ti_{3.3}Al$. The atomic weight of titanium is nearly equal to that of aluminum in location 4; thus the layer III is mainly composed of TiAl. Atomic ratio of titanium to aluminum is approximately 1:2 in location 5. There are $TiAl_2$ in the layer IV; however, the results of XRD have revealed the existence of Ti_5Al_{11} and Ti_9Al_{23} superstructures. So the layer IV may be a mixture of intermetallics $TiAl_2$, Ti_5Al_{11}, and Ti_9Al_{23}. Atomic ratio of titanium to aluminum is approximately 1:3 in location 6; apparently the layer V is composed of $TiAl_3$. A few bright nanoparticles distribute in layers II, III, and IV. The nanoparticles are Ti_5Si_3 according to the observations of XRD. Thus the layer II is a eutectic structure of $Ti_{3.3}Al + Ti_5Si_3$. The layer III is composed of $TiAl + Ti_5Si_3$ eutectic structure. The layer IV may be a mixture structure of intermetallics $TiAl_2$, Ti_5Al_{11}, Ti_9Al_{23}, and Ti_5Si_3.

Based on observations above, the formation mechanism of intermetallics in titanium/aluminum fusion zone could

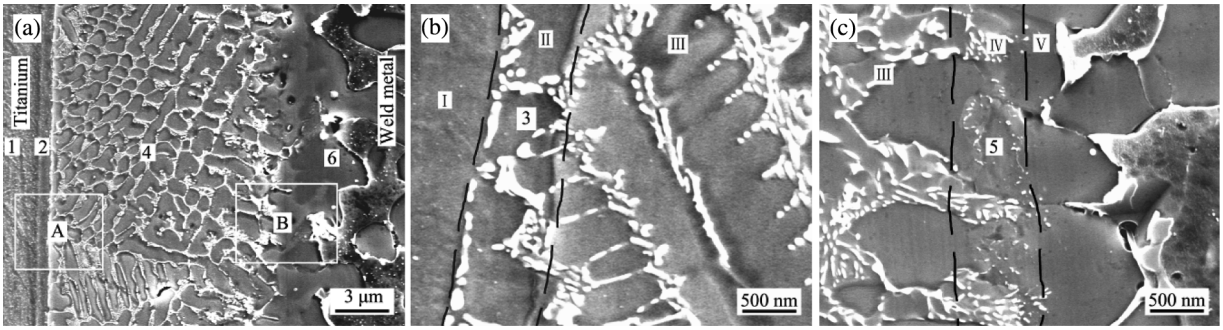

FIGURE 7.—EDS analysis of the titanium/aluminum fusion zone: (a) microstructure of the fusion zone, (b) microstructure of Zone A, and (c) microstructure of Zone B.

TABLE 2.—EDS element analysis at the locations 1–6 in Fig. 7.

Locations	Atomic weight (at%)			
	Ti	Al	Si	V
1	86.62	10.83	—	2.54
2	72.81	24.16	0.67	2.36
3	68.45	28.29	1.33	1.93
4	42.52	46.92	9.77	1.79
5	29.19	61.70	8.44	0.67
6	20.85	72.52	6.63	—

be summarized as following. Surface of titanium was partially melted and mixed with liquid filler metal during the welding–brazing. A titanium-rich zone was formed near solid titanium and an aluminum-rich zone was formed in liquid metal side. Diffusion of aluminum from liquid metal toward solid titanium occurred during the welding–brazing. Because aluminum is a stable element of α-Ti, phase transformation from α-Ti to β-Ti was suppressed by the presence of aluminum [20], and a thin α-Ti layer was formed in the titanium base metal.

Mass weight of silicon in liquid metal was lower than 5 wt%. Intermetallics Ti_3Si and Ti_5Si_3 are the probable products during the welding–brazing according to titanium–aluminum–silicon binary phase diagram [14]. Phase transformations $\beta\text{-Ti} \rightarrow \alpha\text{-Ti} + Ti_3Si$ and $\beta(Ti) + Ti_5Si_3 \rightarrow Ti_3Si$ only take place at a quasi-steady state according to former researches [21, 22]. Thus reactions $L \rightarrow \beta\text{-Ti}$, $L \rightarrow Ti_{3.3}Al + Ti_5Si_3$, $L \rightarrow TiAl + Ti_5Si_3$, $L \rightarrow TiAl_2 + Ti_5Si_3$, $L \rightarrow Ti_5Al_{11}$, $L \rightarrow Ti_9Al_{23}$, and $L \rightarrow TiAl_3$ took place from the titanium-rich side to the aluminum-rich side, and layers with α-Ti, β-Ti, $Ti_{3.3}Al + Ti_5Si_3$, $TiAl + Ti_5Si_3$, $TiAl_2 + Ti_5Si_3 + Ti_5Al_{11} + Ti_9Al_{23}$, and $TiAl_3$ were formed orderly from titanium to the liquid metal. Concentration of aluminum in the β-Ti layer was so high that phase transformation $\beta\text{-Ti} \rightarrow \alpha\text{-Ti} + Ti_{3.3}Al$ took place during the rapid cooling process [14], and a $Ti_{3.3}Al$ layer was formed adjacent to the α-Ti layer.

Microhardness Distribution

Because thick intermetallic layers were formed in the titanium/aluminum fusion zone during the welding–brazing, it is necessary to investigate microhardness distribution crossing the fusion zone. The result of microhardness test is shown in Fig. 8. Microhardness of the titanium base metal is 290–310 $HV_{0.05}$. Temperature of titanium base metal near the titanium/aluminum interface had exceeded 882.5°C during the welding–brazing. Phase transformations $\beta\text{-Ti} \rightarrow \alpha\text{-Ti}$ and $\beta\text{-Ti} \rightarrow \alpha$ martensite took place during the rapid cooling process. Thus the heat-affected zone is composed of α-Ti, α martensites, and retained β-Ti. The heat-affected zone is divided into two regions named the coarse grain zone that is near the fusion zone and the fine grain zone that near the base metal, as shown in Fig. 8(a). Microhardness distribution in the heat-affected zone depends much on the presence of α martensites. Microhardness of the fine grain zone is 320–340 $HV_{0.05}$ for the existence of α martensites. Microhardness of the coarse grain zone is even higher for containing more α martensites, which is 340–360 $HV_{0.05}$. The titanium/aluminum fusion zone is mainly composed of brittle intermetallics. Microhardness of the intermetallic layers is much higher than that of heat-affected zone in titanium, approximately 500 $HV_{0.05}$. The test results of intermetallic layers are close to that reported in other research [16].

The weld metal is composed of α-Al dendrites and α-Al + Si eutectic phases according to EDS analysis. However, $TiAl_3$ precipitations were generated in the weld metal near the titanium/aluminum fusion zone. Microhardness of weld metal near the titanium is 80–90 $HV_{0.05}$ result from the presence of $TiAl_3$ precipitations. Microhardness of weld metal near the aluminum is a little lower, about 70 $HV_{0.05}$.

Microhardness distribution near the fusion zone at aluminum side is shown in Fig. 8(b). The fusion zone is composed of columnar α-Al grains and α-Al + Mg_2Si + silicon eutectic structures. Microhardness of the fusion zone is 80–90 $HV_{0.05}$, which is a little higher than that of weld metal but lower than that of aluminum base metal (110–120 $HV_{0.05}$). Microhardness of the heat-affected zone near the fusion zone is 80–100 $HV_{0.05}$ due to the decomposition of β phase and the diffusion of magnesium into the weld metal. Microhardness of the heat-affected zone away from the fusion zone is close to that of the base metal, approximately 100–120 $HV_{0.05}$.

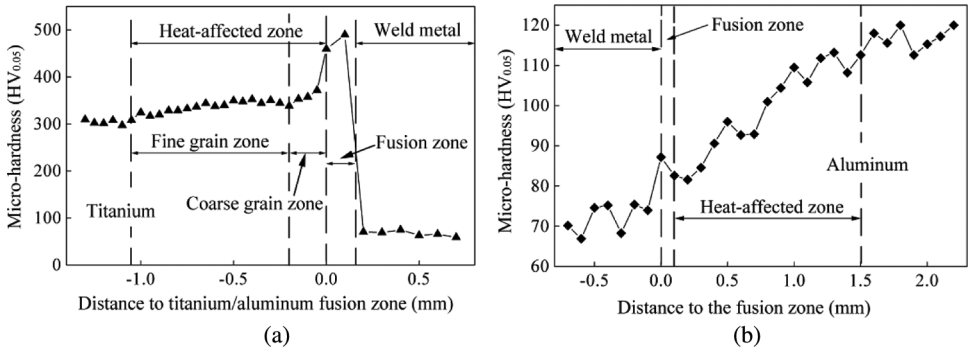

FIGURE 8.—Microhardness distribution in the joint: (a) near titanium/aluminum fusion zone and (b) near fusion zone at aluminum side.

Conclusions

Butt welding of titanium to aluminum was conducted using a novel gas tungsten arc welding–brazing technology. Microstructure characteristics and microhardness distribution in the joint were investigated in detail. Phase constitution of titanium/aluminum reaction zone was studied by means of XRD and energy-dispersive X-ray spectroscopy. Conclusions were summarized in the following based on the analysis of experimental results.

1. Titanium Ti-6Al-2Zr-Mo-1.5V and aluminum Al-5Mg-0.6Mn dissimilar alloys were butt joined using a novel gas tungsten arc welding–brazing technology. Joints without welding defects can be achieved using AlSi5 filler metal. Microstructures of the titanium/aluminum reaction zone were improved by using the novel welding–brazing technology. Fusion welding is observed at the aluminum side. Dual characteristics of fusion welding and brazing are exhibited at the titanium side.
2. Aluminum base metal was partially melted due to the heat conduction from welding arc and liquid filler metal. An obvious fusion zone was formed at Al-5Mg-0.6Mn side. The fusion zone is composed of columnar α-Al grains and α-Al + Mg_2Si + silicon eutectic structures.
3. Top surface of titanium base metal was melted slightly and a thin titanium/aluminum fusion zone was formed in the top of the joint. Five different reaction layers with intermetallics $Ti_{3.3}Al$, $Ti_{3.3}Al + Ti_5Si_3$, $TiAl + Ti_5Si_3$, $TiAl_2 + Ti_5Si_3 + Ti_5Al_{11} + Ti_9Al_{23}$, and $TiAl_3$ were formed in the fusion zone orderly from titanium side to the weld metal. Microhardness of the titanium/aluminum fusion zone was very high due to the intrinsic brittleness of intermetallics.
4. Titanium stayed in solid state in other regions during the welding–brazing process. An unequal-thickness reaction zone was formed near the titanium/aluminum-brazed interface due to the interaction between the solid titanium with liquid metal. Two reaction layers with intermetallics $Ti_7Al_5Si_{12}$ and $TiAl_3$ were formed in the reaction zone.

Funding

This research was financially supported by the National Natural Science Foundation of China (No. 51175303). The authors express heartfelt thanks here.

References

1. Chen, Y.B.; Chen, S.H.; Li, L.Q. Effects of heat input on microstructure and mechanical property of Al/Ti joints by rectangular spot laser welding–brazing method. *International Journal of Advanced Manufacturing Technology* **2009**, *44*, 265–272.
2. Chen, G.Q.; Zhang, B.G.; Liu, W.; Feng, J.C. Crack formation and control upon the electron beam welding of TiAl-based alloys. *Intermetallics* **2011**, *19*, 1857–1863.
3. Kothari, K.; Radhakrishnan, R.; Wereley, N.M.; Sudarshan, T.S. Rapid consolidation of gamma titanium aluminide powders attrition milled to submicron scale. *Materials and Manufacturing Processes* **2013**, *28*, 1171–1178.
4. Majumdar, B.; Galun, R.; Weisheit, A.; Mordike, B.L. Formation of a crack-free joint between Ti alloy and Al alloy by using a high-power CO_2 laser. *Journal of Materials Science* **1997**, *32*, 6191–6200.
5. Chen, X.G.; Yan, J.C.; Ren, S.C.; Wei, J.H.; Wang, Q. Microstructure and mechanical properties of Ti-6Al-4V/Al1060 joints by ultrasonic-assisted brazing in air. *Materials Letters* **2013**, *95*, 197–200.
6. Song, Z.H.; Nakata, K.; Wu, A.P.; Liao, J.S. Interfacial microstructure and mechanical property of Ti6Al4V/A6061 dissimilar joint by direct laser brazing without filler metal and groove. *Materials Science and Engineering: A* **2013**, *A560*, 111–120.
7. Mirjalili, M.; Soltanieh, M.; Matsuura, K.; Ohno, M. On the kinetics of $TiAl_3$ intermetallic layer formation in the titanium and aluminum diffusion couple. *Intermetallics* **2013**, *32*, 297–302.
8. Kenevisi, M.S.; Mousavi Khoie, S.M.; Alaei, M. Microstructural evaluation and mechanical properties of the diffusion bonded Al/Ti alloys joint. *Mechanics of Materials* **2013**, *64*, 69–75.
9. Chen, Y.C.; Nakata, K. Microstructural characterization and mechanical properties in friction stir welding of aluminum and titanium dissimilar alloys. *Materials & Design* **2009**, *30*, 469–474.
10. Dressler, U.; Biallas, G.; Alfaro Mercado, U. Friction stir welding of titanium alloy TiAl6V4 to aluminium alloy AA2024-T3. *Materials Science and Engineering: A* **2009**, *A526*, 113–117.
11. Kreimeyer, M.; Florian, W.; Frank, V. Laser Processing of aluminum–titanium-tailored blanks. *Optics and Lasers in Engineering* **2005**, *43*, 1021–1035.
12. Vaidya, W.V.; Horstmann, M.; Ventzke, V.; Petrovski, B.; Kocak, M.; Kocik, R.; Tempus, G. Improving interfacial properties of a laser beam welded dissimilar joint of aluminium AA6056 and titanium Ti6Al4V for aeronautical applications. *Journal of Materials Science* **2010**, *45*, 6242–6254.
13. Lv, S.X.; Jing, X.J.; Huang, Y.X.; Xu, Y.Q.; Zheng, C.Q.; Yang, S.Q. Investigation on TIG arc welding–brazing of Ti/Al dissimilar alloys with Al based fillers. *Science and Technology of Welding and Joining* **2012**, *17* (7), 519–524.
14. Sambasiva Rao, A.; Madhusudhan Reddy, G.; Satya Prasad, K. Microstructure and tensile properties of dissimilar metal gas tungsten arc welding of aluminium to titanium alloy. *Materials Science and Technology* **2011**, *27* (1), 65–70.
15. Ma, Z.P.; Wang, C.G.; Yu, H.C.; Yan, J.C.; Shen, H.R. The microstructure and mechanical properties of fluxless gas tungsten arc welding–brazing joints made between titanium and aluminum alloys. *Materials & Design* **2013**, *45*, 72–79.
16. Shant, P.G. Intermetallic compounds in diffusion couples of Ti with an Al–Si eutectic alloy. *Materials Characterization* **2003**, *49*, 321–330.
17. Chen, S.H.; Li, L.Q.; Chen, Y.B.; Liu, D.J. Si diffusion behavior during laser welding–brazing of Al alloy and Ti alloy with Al-12Si filler wire. *Transactions of Nonferrous Metals Society of China* **2010**, *20*, 64–70.

18. El-Danaf, E.A.; Soliman, M.S.; Almajid, A.A. Effect of solution heat treatment on the hot workability of Al–Mg–Si alloy. *Materials and Manufacturing Processes* **2009**, *24*, 637–643.
19. Wei, S.Z.; Li, Y.J.; Wang, J.; Zhang, P.F. Microstructure and joining mechanism of Ti/Al dissimilar joint by pulsed gas metal arc welding. *International Journal of Advanced Manufacturing Technology* **2014**, *70*, 1137–1142.
20. Chen, S.H.; Li, L.Q.; Chen, Y.B.; Huang, J.H. Joining mechanism of Ti/Al dissimilar alloys during laser welding–brazing process. *Journal of Alloys and Compounds* **2011**, *509*, 891–898.
21. Antonova, N.; Firstov, S.A.; Miracle, D.B. Investigation of phase equilibria in the Ti-Al-Si-Nb system at low Nb contents. *Acta Materialia* **2003**, *51*, 3095–3107.
22. Zhan, Y.Z.; Zhang, X.J.; Hu, J.; Guo, Q.H.; Du, Y. Evolution of the microstructure and hardness of the Ti-Si alloys during high temperature heat-treatment. *Journal of Alloys and Compounds* **2009**, *479*, 246–251.